Mucus permeating thiolated self-emulsifying drug delivery systems

Julia Rohrer[1], Alexandra Partenhauser[1], Sabine Hauptstein[1], Caroline Marie Gallati[2], Barbara Matuszczak[2], Muthanna Abdulkarim [3], Mark Gumbleton[3], Andreas Bernkop-Schnürch[1]*

[1]Department of Pharmaceutical Technology, Institute of Pharmacy, University of Innsbruck, Innrain 80/82, Innsbruck, Austria

[2]Department of Pharmaceutical Chemistry, Institute of Pharmacy, University of Innsbruck, Innrain 80/82, Innsbruck, Austria

[3]School of Pharmacy and Pharmaceutical Sciences, Cardiff University, Cardiff CF10 3NB, UK

**Corresponding author: Andreas Bernkop-Schnürch, Department of Pharmaceutical Technology, Institute of Pharmacy, University of Innsbruck, Innrain 80/82, Innsbruck, Austria. Tel: +43 51250758601; Fax: +43 51250758699. E-mail: andreas.bernkop@uibk.ac.at*

Key Words: mucolytic, low molecular weight thiolated compounds, fatty acid derivatives

Graphical abstract

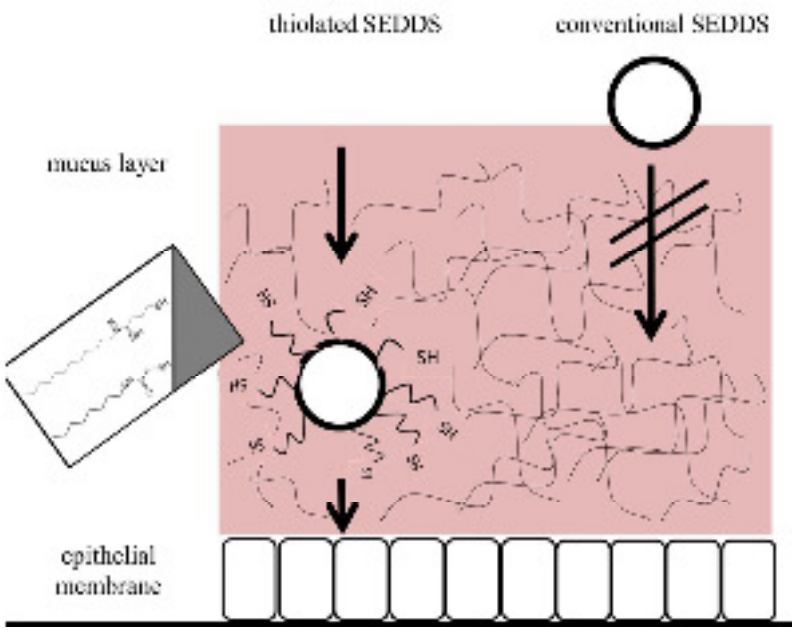

Abstract

Context: Mucus represents a critical obstacle for self-emulsifying drug delivery systems (SEDDS) targeting the epithelial membrane site.

Objective: The aim of the study was the development of a novel SEDDS to overcome the mucus barrier.

Materials and methods: Two novel conjugates *N*-dodecyl-4-mercaptobutanimidamide (thiobutylamidine-dodecylamine, TBA-D) and 2-mercapto-*N*-octylacetamide (thioglycolic acid-octylamine, TGA-O) were synthesized, incorporated into SEDDS and analysed for stability, cytotoxicity and physico-chemical characteristics using dynamic light scattering. Mucus interaction studies were performed using *in vitro* assays based on multiple particle tracking, rotational silicone tubes and rheology.

Results and discussion: TBA-D was synthesized using dodecylamine and iminothiolane as thiol precursor (yield=55±5%). TGA-O was obtained via crosslinking of octylamine with SATA ((2,5-dioxopyrrolidin-1-yl) 2-acetylsulfanylacetate) (yield=70±6%). The chemical structure of target compounds was confirmed via NMR analysis. The thiol-conjugates were incorporated in an amount of 3% (m/m) into SEDDS (Cremophor EL 30%, Capmul MCM 30%, Captex 355 30% and propylene glycole 10%), namely thiolated SEDDS leading to a droplet size around 50 nm and zeta potential close to 0 mV. Thiolated SEDDS with an effective diffusion coefficient ‹Deff› of up to 0.871 ± 0.122 $cm^2s^{-1}x10^{-9}$ were obtained. Rotational silicone studies show increased permeation of the thiolated SEDDS A in comparison to unthiolated control. Rheological studies confirmed the mucolytic activity of the thiol-conjugates which differed only by 3 % from DTT (dithiothreitol) serving as positive control.

Conclusion: Low molecular weight thiol-conjugates were identified to improve the mucus permeation, leading to highly efficient mucus permeating SEDDS, which were superior to conventional SEDDS and might thus be a new carrier for lipophilic drug delivery.

1. Introduction

Mucus protects the various mucosal surfaces of the body and represents a major hindrance for particulate drug delivery to the underlying mucosal epithelium [1–3]. The mucus hydrogel forms a steric barrier and promotes clearance of pathogens, e.g. viruses, trapped within the mucus network network [2,4,5]. Similarly drug carriers that are incapable of diffusing fast enough through the mucus are held within the adhesive network and degraded prior to their delivery to the target absorptive epithelial membrane site [1–4]. Permeating the mucus barrier is a major requirement for successful drug targeting to mucosal tissues. Several strategies to overcome the mucus barrier were recently summarized by Dünnhaupt [6]. Nano particulate systems, bearing enzymatically active compounds or systems possessing a 'slippery surface', as well as 'zeta-potential changing systems' are described in literature[7–10]. Among various approaches, SEDDS emerged to have beneficial features to overcome the mucosal barrier. As shown by Friedl et al. [11], the composition of SEDDS has great impact on their mucus permeating properties. SEDDS consist of an oily phase, containing oil(s), a surfactant(s) and co-surfactant that emulsifies spontaneously upon mixing in an aqueous environment [12,13]. The resulting droplets are typically in the nanometer scale (< 100 nm) favorable for the diffusion through mucus as the mucus is reported to express 50% of its pores below a size of 200 nm [14,15]. As the dynamic properties of mucus remain a considerable challenge for drug targeting, novel mucus permeating systems are needed.

The aim of the study was the development of a novel mucus permeating system based around thiolated SEDDS. The strategy was to equip a nano-emulsion with thiol-moieties that are likely to interact with mucus, leading to a destruction of disulfide bonds of mucus network. This could be realized by the design of a series of novel thiolated emulsifiers based on modified fatty acid derivatives, which structure identification was assessed via NMR. Ease of incorporation of the novel highly lipophilic thiol-conjugates into SEDDS led to stable

thiolated oil-in-water nano-emulsions which were spontaneously formed upon dilution in aqueous environment, namely thiolated SEDDS.

The novel thiolated SEDDS were evaluated for their cytotoxicity and their muco-interactive features. Mucus permeating capacity of the novel designed thiolated SEDDS was evaluated using common *in vitro* models based on multiple particle tracking and on rotating silicone tubes. Mucolytic activity of the novel thiolated conjugates was studied using *in vitro* rheological measurements. In addition, computational predictions of the partition coefficient of the novel thiolated conjugates were provided.

2. Materials and Methods

2.1. Materials

Dodecylamine was purchased from Merck Millipore, Austria. Iminothiolane hydrochloride and SATA ((2,5-dioxopyrrolidin-1-yl) 2-acetylsulfanylacetate) were purchased from Santa Cruz, Biotechnology Heidelberg, Germany. Cremophor EL was purchased from BASF, Germany. Captex 355 and Capmul MCM were obtained from Abitec Corporation, United States. Propylene glycole was obtained from Gatt-Koller, Absam Austria. Fluoresceindiacetate (FDA) and N-acetylcysteine (NAC) and DTT (dithiothreitol) were purchased from Sigma-Aldrich, Austria. MEM (minimal essential medium) with and without phenol red was purchased from Sigma-Aldrich, Austria. Lumogen ® dye was bought from Kremer, Germany. All other chemicals were of analytical grade and from commercial sources. Silicone tubes were obtained from Lactan, Austria.

2.2. Methods

2.2.1. Synthesis of thiolated conjugates

Synthesis of TBA-D

In a round bottom flask 1.816 mmol dodecylamine (1 eqv), 1.816 mmol iminothiolane hydrochloride (1 eqv) and 1.998 mmol triethylamine (1.1eqv) were dissolved in a mixture of 10 ml acetonitrile and 4 ml methanol. The solution was stirred at room temperature for approximately 4 h and the solvent was removed under reduced pressure. The crude product was purified via chromatography over silica as stationary phase and diethyl ether 100% as mobile phase to yield the product as a colorless liquid (yield = 55±5%) (Figure 1A). Finally the product was stored under inert gas at -20 °C until further use.

Synthesis of TGA-O

In the first reaction step, 2 mmol octylamine (1 eqv), 2 mmol SATA (1 eqv) and 0.2 mmol triethylamine (0.1 eqv) were dissolved in 10 ml acetonitrile in a round bottom flask. The

solution was stirred at room temperature and monitored with thin layer chromatography. After 2.5 h, the solvent was removed under reduced pressure. The crude product was purified via chromatography over silica as stationary phase using a mixture of petroleum ether and ethyl acetate (7:3) as mobile phase to yield the protected thioester (product A) as a white solid (Figure 1B). In the second step the thioester was hydrolysed by suspending TGA-octylamine-thioester, hydroxylamine hydrochloride, EDTA (2,2',2",2"'-(ethane-1,2-diyldinitrilo)tetraacetic acid) and sodium hydrogen carbonate in a mixture of water and methanol (1:1). The pH was adjusted to pH 7 and the suspension was stirred at room temperature under thin layer chromatographic monitoring. After approximately 3 h, when the reaction had reached completion the product was extracted with dichloromethane. The organic phases were combined and dried with anhydrous sodium sulfate and the solvent was removed under reduced pressure. The product was purified via chromatography over silica as stationary phase using a mixture of dichloromethane and ethyl acetate (6:4) as mobile phase to yield the TGA-O as a colorless liquid (yield = 70±6%). Finally the product was stored under inert gas at -20°C until further use.

2.2.2. Identification of thiolated compounds: NMR analysis

The thiol conjugates were analyzed by ^{1}H and ^{13}C NMR spectra (Varian Gemini 200 spectrometer (^{1}H: 199.98 MHz, ^{13}C: 50.29 MHz). The center of the solvent multiplet ($CDCl_3$) was used as internal standard, which was related to TMS δ=7.26 ppm for ^{1}H and δ=77.00 ppm for ^{13}C.

2.2.3. Formulation of SEDDS

The new thiol-conjugates TBA-D and TGA-O were incorporated in a SEDDS-formulation previously developed by our research group [16]. The original SEDDS formulation consists of Cremophor EL 30%, Capmul MCM 30%, Captex 355 30 % and propylene glycol 10 %. The SEDDS preconcentrate was spiked with 3 % (m/m) of thiol-conjugate referring exemplarily to NAC as control. The other thiol-conjugates, TBA-D and TGA-O, were incorporated in an

equivalent molar amount. This results of course in different masses of the thiol-conjugates due to their different molecular masses. NAC was chosen, as it is reported to be the most commonly used mucolytic agent and provides only one thiol moiety on the molecule and is thus best comparable to the novel thiol conjugates. The prepared liposolution consisting of emulsifier, lipid phase and co-solvent was thoroughly mixed to guarantee a homogeneous formulation and then diluted with 0.1 M bis-tris-buffer of pH 6.8 in a ratio of 1:100.

2.2.4. SEDDS characterisation

The stability of SEDDS was confirmed via a centrifugation test of 12,100 g for 20 min using minispin centrifuge, Eppendorf, Germany. In addition, the particle size was monitored prior to experiment via an extended shelf-life study up to 12h using bis-ris buffer pH 6.0, 0.1M in a 1:100 dilution. To estimate stability of SEDDs in cell culture medium, preliminary tests were performed exemplarily for SEDDS A using white MEM as dispersing agent.

Size, zeta potential and polydispersity index of SEDDS formulations were determined by photon correlation spectroscopy using Nicomp PSS 380 DLS/ZLS, Particle Sizing Systems, Inc. Port Richey, Florida with a laser wavelength of 650 nm and an E-fields strength of 5 V/cm. The experiment was performed at room temperature.

2.2.5. Cell viability assay- resazurin assay

The potential cytotoxic effect of the thiolated SEDDS was evaluated using the resazurin assay on a human colon carcinoma cell line monolayer according to a protocol previously reported by our research group [17]. Caco-2 cells were cultured over a period of 14 days in 24-well plates. After seeding the cells (d=25 x 10^3 cells/well) they were fed with 500 µl of minimal essential medium (MEM) supplemented with 20% fetal bovine serum (FBS) at 37 °C in 5% CO_2 environment. Every second day the medium was replaced by fresh medium. The assay was performed with resazurin which is reduced to fluorescent resorufin. Before incubating the cells with the test medium, they were washed with 500 µl of phosphate buffered saline (PBS) and then incubated with 500 µl of 0.5% sample solution (prepared with white MEM, which

consists of MEM omitting the indicator). After incubating the samples for 4 hours, the cells were washed again with PBS and were incubated with 250 µl of resazurin solution 44 µM for another time period of 3 hours. Cells with MEM as positive control and Triton X 100 as negative control were treated in the same way. 24-well plates omitting the cells were spiked with resazurin and served as blank. Aliquots of the samples were transferred to a microtiter plate and the fluorescence intensity was measured using a microplate reader (Tecan; Groedig; Salzburg, Austria) at a excitation wavelength of λ_{exc} = 540 nm and an absorption wavelength of λ_{em} = 590 nm. The cell viability was calculated based on to the positive control with white MEM [18]

$$\frac{\text{fluorescence of cells treated with samples}}{\text{fluorescence of cells treated with white MEM}} \times 100.$$

2.2.6. *In vitro* mucus permeation studies

Mucus refinement

Freshly isolated pig intestinal ileum (5 m length from proximal region) was obtained from a local abattoir and kept in ice-cold oxygenated phosphate buffered saline (PBS) prior to sample processing. The ileum was processed into 25 cm lengths with each length then incised longitudinally. Food and other waste debris were gently rinsed away by ice-cold PBS. The mucus was then gently scraped from the intestinal surface with a spoon to avoid excessive shedding of intestinal epithelial tissue. Mucus was divided into aliquots (0.5 g) and kept at -20 °C prior to experimentation [19].

2.2.6.1. *In vitro* permeation study- multiple particle tracking (MPT) in mucus

The effect of thiolated compounds on droplets permeation within mucus was studied using MPT technique according to a protocol reported previously [15]. Therefore, the formulations were labelled with the fluorescent dye Lumogen ®. Diffusion of SEDDS droplets through intestinal mucus was assessed by MPT [20] a technique that can track particle displacement with a tracking resolution (σ) to within 5 nm [21]. In this study the ‘tracking resolution’ (σ)

was experimentally determined for each SEDD particle type. Specifically, σ was measured by gluing (cyanoacrylate-based glue) the particles to a glass bottom imaging dish followed by drying and setting of the glue matrix and video microscopy capture (ImageJ) of particles fluorescence. The σ was then calculated by two approaches: (i) independently determining X- and Y-direction fluorescence displacement at lowest temporal resolution (33 ms) followed by calculation of geometric mean of the data; (ii) Calculation of square root of MSD at lowest temporal resolution, with MSD calculated as below. Both approaches gave the same σ data of: SEDDS A 4.8 nm; SEDDS B 4.6 nm; SEDDS C 4.7 nm; SEDDS NAC 4.8 nm. Overall the σ was confirmed at 5 nm for the SEDD formulations.

For the mucus permeation studies samples (0.5 g) of porcine intestinal mucus were incubated in glass-bottom MatTek imaging dishes at 37 °C. The fluorescently labelled droplets were inoculated into each 0.5 g mucus sample in a 25 µl aliquot. To ensure effective droplet distribution within the matrix a 2 hours period of equilibration was allowed following inoculation and prior to video microscopy capture of droplets movement within the mucus. Video capture involved 2-dimensional imaging on a Leica DM IRB wide-field epifluorescence microscope (x63 magnification oil immersion lens) using a high speed camera with a 20 x digital magnification system (Allied Vision Technologies, UK) running at a frame rate of 33 ms i.e. capturing 30 frames sec^{-1}; each completed video film comprised 300 frames. For each 0.5 g of mucus sample approximately 120 droplets were simultaneously tracked and their movements captured. For any distinct droplets species a minimum of three distinct mucus samples were analysed, i.e. minimum of 360 individual droplets trajectories assessed. Videos were imported into Fiji ImageJ software which converts the movement of each droplet into individual droplets trajectories across the full duration of the 10 seconds (300 frames). The the movement of each particle within sequential 30 frame segments (corresponding to 1 s intervals) is then analysed, i.e. we collect data on a single particle over a 10 s period and calculate 270 individual movements. One criterion applied is that for

inclusion in the sequential analysis the droplet must have displayed a continuous presence in the X-Y plane for the 30 sequential frames. This limits the impact of mucin movement upon the droplet diffusion calculations [22]. The individual droplet trajectories were converted into numeric pixel data (Mosaic Particle Tracker within Fiji ImageJ). This data was then converted from pixels into metric distance based on the microscope and video capture settings. The distances moved by each droplet over a selected time interval (Δt) in the X-Y trajectory were then expressed as a squared displacement (SD). The mean square displacement (MSD) of any single droplet (*n*) represents the geometric mean of the droplet's squared displacements throughout it is entire 30-frame trajectory. The MSD was determined as follows [23]:

$$MSD_{(n)} = (X_{\Delta t})^2 + (Y_{\Delta t})^2 \quad (1)$$

In any single experiment an MSD was calculated for at least 120 individual droplets with the experiment replicated a further two times, i.e. 360 droplets studied in total. For each droplets species under study an "ensemble mean square displacement" (defined by ‹MSD›) was determined for each of the three replicate studies.

The **effective diffusion coefficient** (‹Deff›) for a particular droplets species was then calculated by:

$$\text{‹Deff›} = \text{‹MSD›}/(4 * \Delta t) \quad (2)$$

where 4 is a constant relating to a 2-dimensional mode of video capture and Δt is the selected time interval.

Proportion of diffusive droplets: Measuring droplet diffusion across various time intervals allows description of the proportion of droplets that are diffusive through the mucus matrix [22]. Equation 3 was used to determine a diffusivity factor (DF) which expresses the effective diffusion coefficient for each individual droplet (Deff) across the time intervals (*Δt*) of 1 s and 0.2 s

$$DF = Deff_{\Delta t=1\ s} / Deff_{\Delta t=0.2\ s} \quad (3)$$

where the individual droplet Deff = MSD/(4 * Δt). Droplets with a DF value of 0.9 and greater were defined as diffusive. The proportion of diffusive droplets within a given droplets type was then calculated and expressed as % Diffusive droplets.

Heterogeneity in droplet diffusion: Profiling the diffusive properties of each droplet within an entire population provides information on the heterogeneity of droplet movement and the presence of outlier sub-populations indicative of distinctive pathways of diffusion through the matrix. Here the effective diffusion coefficient for each individual droplet (Deff) was calculated at the time interval (Δt) of 1 s, and for any droplets type all 360 $Deff_{\Delta t=1\ s}$ were then ranked to allow comparison of the highest (90^{th}) and lowest (10^{th}) percentiles, where for example the 90^{th} percentile is the Deff value below which 90% of the Deff observations may be found.

Droplet diffusion in water: The droplets' diffusion coefficient (D°) in water was calculated by the Stokes-Einstein equation at 37 C° [24]:

$$[D° = \kappa T / 6\pi\eta r] \quad (4)$$

where κ is Boltzmann constant, *T* is absolute temperature, η is water viscosity, r is radius of the droplet. The diffusion of all droplets was also expressed as the parameter, % ratio [Deff] / [D°].

2.2.6.2. *In vitro* mucus diffusion study- rotating tube method

The permeation study was performed according to a protocol previously reported by our research group [25]. In brief, silicon tubes (Ø=3 mm) were filled with a volume of 200 µl of mucus and closed at one end, then 50 µl of formulation was applied to the open end of the tube and then closed using silicone plug. Formulation was labeled with 0.3% fluoresceine diacetate and diluted in a 1:100 dilution of bis-tris-buffer (0.1M) pH 6. The tubes were placed in an incubator with a rotating device at gentle rotation for a time period of 4 hours at 37 °C.

Then the samples were frozen at -80°C for at least 1 hour. Then the tubes were cut- starting from the point where the mucus was added- into 10 slices of 2 mm each, and to each slice of mucus containing sample 300 µl of 5 M sodium hydroxide solution were added. In order to activate the fluorescent dye, the slices were incubated for 6 hours and fluorescence was measured at a wavelength of λ_{exc} = 480 nm and λ_{em} = 520 nm with a microplate reader (Tecan; Grödig; Salzburg, Austria). The amount of fluorescein diacetate in each slice was quantified using a standard calibration curve. Samples containing only mucus were additionally analysed- serving as blank. The experiment was performed in quintuplicate.

2.2.7. In vitro study of mucolytic activity

Mucolytic activity was assessed according to a technique previously reported by our research group using a plate-plate combination rheometer (Haake Mars Rheometer, 379-0200, Thermo Electron GmBH, Karlsruhe, Germany; Rotor: PP35, D=35 mm) [26]. After determining the linear viscoelastic region of the gels using the oscillating modulus, the shear stress rate was set to a range of 0.1-2 Pa, with a frequency of 1 Hz at a temperature of 37±1°C and the gap between two plates was chosen about 0.5 mm. The rheological study was performed with the pure thiol-conjugates TBA-dodecylamine and TGA-octylamine using DTT as positive control. An ethanolic solution of 30 µmol, in reference to the thiol groups of each respective conjugate, was dissolved in 100µl of EtOH and mixed with mucus in a ratio of 1:10 (V/m). Mucus, diluted with the same amount of EtOH and treated the same way as the samples served as 100 % control for each respective time point. Samples were stored air tight at 37±1°C until rheological analysis was performed. Each measurement was done in quintuplicate.

2.3. Statistical data analysis

Statistical data analysis was performed using the student t-test with $p < 0.05$ as the minimal level of significance. The results are expressed as the means of at least 3 experiments ± SD."

3. Results and discussion

3.1. Synthesis and characterization of the thiolated conjugates

The successful coupling of the thiol ligand was supported by NMR analysis. Neither NMR nor thin layer chromatography indicated impurity. The protons of TBA-D, bond to heteroatoms are not seen in the ^{1}H-NMR (Appendix A). The formation of the amidine bond is confirmed by the signal at 172.2 ppm attributed to the amidine carbon (Appendix B). The first coupling reaction of TGA-O yields to the acetylated product. In the ^{1}H-NMR you can recognize the acetylic group at 2.41 ppm together with a signal at 3.52 ppm corresponding to the methylene group connected to the sulfur atom (Appendix C). After the deprotection step, the signal referred to the acetyl group lacks, confirming that the reaction was successful (Appendix D). At 1.85 ppm a triplet appears corresponding to the thiol group and the singlet at 3.52 ppm is replaced by a signal of higher multiplicity included in the multiplet 3.22-3.33 ppm. In both spectra it is possible to see the proton connected to the nitrogen at 6.19 ppm and 6.69 ppm.

The structure of the products was confirmed by NMR spectroscopy (see Appendix A-E). ***TBA-D ^{1}H-NMR*** *($CDCl_3$)*: δ 0.88 (t, 3H, CH_3, J = 6.4 Hz), 1.20-1.40 (m, 18H, $(CH_2)_9$), 1.59-1.75 (m, 2H, C**H**$_2$CH$_2$NH), 2.03-2.17 (m, 2H, C**H**$_2$CH$_2$SH), 2.61-2.69 (m, 2H), 3.13-3.25 (m, 4H), (C**H**$_2$NH, C**H**$_2$CH$_2$C**H**$_2$SH).

^{13}C-NMR *($CDCl_3$)*: δ 14.30 (CH_3), 22.87 (CH_2), 27.08 (CH_2), 27.78 (CH_2), 29.53 (CH_2), 29.68 (CH_2), 29.80 (CH_2), 29.82 (CH_2), 29.85 (CH_2), 30.64 (CH_2), 32.10 (CH_2), 33.80 (CH_2), 38.93 (CH_2), 58.17 (C-N); 172.24 (C=N).

TGA-O-Thioester ^{1}H-NMR *($CDCl_3$)*: δ 0.88 (t, 3H, CH_3, J = 6.4 Hz), 1.18-1.35 (m, 10H, $(CH_2)_5$), 1.41-1.55 (m, 2H, CH_2), 2.41 (s, 3H, CH_3), 3.21 (q, 2H, C**H**$_2$NH, J = 6.6 Hz), 3.52 (s, 2H, COCH$_2$S), 6.19 (s (br), 1H, NH).

TGA-O ^{1}H-NMR *($CDCl_3$)*: δ 0.88 (t, 3H, CH_3, *J* = 6.4 Hz), 1.20-1.40 (m, 10H, $(CH_2)_5$), 1.46-1.60 (m, 2H, CH_2), 1.85 (t, SH, *J* = 9.2 Hz), 3.22-3.33 (m, 4H, C**H**$_2$NH, COC**H**$_2$SH), 6.69 (s (br), 1H, NH).

^{13}C-NMR *($CDCl_3$)*: δ 14.27 (CH_3), 22.80 (CH_2), 27.06 (CH_2), 28.51 (CH_2), 29.35 (CH_2), 29.40 (CH_2), 29.59 (CH_2), 31.95 (CH_2), 40.13 (CH_2NH), 169.08 (C=O).

3.2. Preparation, stability and characterization of SEDDS

After 20 min at 12,100 g no visible phase separation could be detected. In addition, the extended shelf-life study as shown in Figure 3 demonstrated, that the size of the droplets remains stable over 12 h. The polydispersity index and the zeta potential showed no significant change in respect to time point zero. In addition, preliminary tests which were performed exemplarily for SEDDS A using white MEM as dispersing agent ensure particle size of approximately 38.2 nm. As shown in Figure 3, droplet size measurements showed a diameter ranging from 36.91 nm to 53.39 nm which is smaller than the mucus average pore size, being reported to range from 20-200 nm [22,27,28]. The incorporation of the thiolated compounds led to no change in size. In addition, the influence on the surface charge is quite limited as the surface charge of the measured formulations was between -0.8 ± 0.9 mV and -7.1 ± 0.2 mV (see Table 1). Cytotoxicity studies on CaCo-2 cell monolayer proved cell viability of the SEDDS formulations of at least 90 % over a time period of 6 hours, indicated by reduction of resazurin to fluorescent resorufin by viable cells (Figure 2) [18].

3.3. In vitro permeation studies

3.3.1. Multiple particle tracking (MPT) in mucus

Incorporation of the thiolated compounds led to an increase in ‹Deff›, which is most pronounced for the formulation termed SEDDS A, with a 66-fold increase (Table 1) in ‹Deff›,

compared to the non-thiolated SEDDS C. Plotting the ‹Deff› versus droplet size (Figure 3) indicates that droplet per se is not the primary determinant of this improved ‹Deff› and that steric obstruction is unlikely to be influential in the diffusion of any of the SEDDS formulations. The SEDDS droplets's sizes were smaller than the average mucus pore size, which is reported to be in the range of 20-200nm [22,27,28]. The porcine mucus, commonly used in in-vitro models, was harvested in a way to collect the loose and the adherent mucus layers. According to Abdulkarim et al., this technique leads to a median pore size of within the mucus mesh of ca. 200 nm with greater than 90% of the pores larger than 100 nm [15]. Additionally, electric or ionic interactions seem to have little to no significant influence on the ‹Deff›. All SEDDS, even the SEDDS C as negative control, which was not containing any thiol-compound, showed motility in the mucus. This might be explained by the fact that a neutral or slightly negative surface charge is favorable for particles to pass through the mucin fiber network [22,27,29,30]. Although the work of Allen et al. [29] refers to gastric and not intestinal mucus, the results are in agreement with the literature [29]. The formulations, used within this study fulfill this fundamental requirement as no hindrance due to ionic interaction, for example, with negatively charged mucoglycoproteins can be detected. Some viruses are reported to be highly efficient mucus permeating, an essential feature for their highly infective potential [31]. The ‹Deff› obtained for thiolated SEDDS A in this study is superior to the diffusion data (assessed using the same model system) obtained for capsid adenoviruses (146 nm diameter) by some 20-fold [15].

The ratio of ‹Deff› to D° provides a measure of the efficiency of the diffusion of the droplets through mucus after the size of the droplet is account for. The ratio normalizes for the droplet's intrinsic free Brownian motion in water and as such the impact of droplet size upon free diffusion. Here the D° is calculated from the Stokes-Einstein equation and given the equivalency of droplet size across the SEDDS formulations (36 to 44 nm; Table 1) the D°

values were similar for all tested formulations (Table1). As such the conclusions that can be derived for the ‹Deff›/D° ratio varied little from that of the findings with the absolute ‹Deff› parameter as discussed above.

The fraction of SEDD droplets, or indeed any particles, that are truly diffusive within the mucus network is a major requirement as immobilization within the in-vivo barrier will lead to droplet clearance away from the target epithelial membrane. Comparing individual droplet diffusion across various time intervals, i.e. across the time intervals (Δt) of 0.2 s and 1 s, allows a description of the proportion of droplets that are truly diffusive. A consistency in Deff across the 1s interval to that in the initial 0.2 s interval reveals the droplets o have minimal interaction with the micro-domains of the mucin network [15,22]. Figure 4 illustrates the Deff profiles for each of 20 randomly selected droplets for the formulations SEDDS A and SEDDs C across the aforementioned time intervals; the SEDDS A formulation contained TBA-D while the SEDDS C formulation lacks a thiolated compound. The profiles clearly show a greater proportion of SEDDS C formulation droplets failing to meet the definition of ‘diffusive’. The DF data for the SEDDs are shown in Table 1, and show consistency with the overall population ‹Deff› data. Specifically, the SEDDS A formulation showed a considerably greater DF than any of the other droplet formulations with 59% of the SEDDS A droplets defined as diffusive compared to only 16% for the control SEDDS C formulation. The DF data obtained for all thiolated SEDDs in this study exceeded the DF data (assessed using the same model system) previously reported for capsid adenoviruses (19%) and by PEGylated particles (32%) [15].

Further analysis of the heterogeneity in diffusion within each of the SEDD formulations was undertaken whereby the Deff for each individual droplet within a formulation was determined and the resulting Deff measurements ranked into percentiles (Figure 5). A more detailed analysis of the heterogeneity in the movement of individual droplets through mucus can

provide insight into how different droplet subpopulations within a given formulation type may exploit divergent permeation pathways [15]. Of the thiolated SEDDS, formulation A was the more homogenous in terms of droplet diffusion with an approximate 20-fold difference between 90^{th} percentile (i.e. the Deff value below which 90 % of the Deff observations may be found) and 10^{th} percentile (i.e. the Deff value below which 10 % of the Deff observations may be found); the SEDDS B and SEDDS NAC formulations showed approximately 60 and 100-fold differences. The non-thiolated formulation, SEDDS C, show a much higher degree of heterogeneity (x1000-fold different) with only 60% of the particles showing negligible to no movement in the mucus. Even the fastest sub-populations of droplets for SEDDS C were below the median rates seen for SEDDS A.

3.3.2. In vitro mucus diffusion study- rotating tube method

The second evaluation of mucus-droplet interaction was done with a static in-vitro model. Therefore, diffusion of SEDDS was assessed using a setup of rotating silicone tubes filled with mucus and using FDA as model drug. The study supported aforementioned data with significant advanced permeation of SEDDS A in respect to control SEDDS C omitting any thiol-conjugate ($p < 0.05$) (Figure 6). The diffusion profile reported, follows a first order kinetics, and the SEDDS containing TBA-D show a significant increased concentration of FDA in comparison to SEDDS C within the first three slices. The negative control, being represented by SEDDS C did not show any significant permeation of droplets than in slice 3. The silicone tube test results were conclusive to the data obtained from MPT technique, although different fluorescent dyes were used and different experimental set-up were performed.

3.4. In vitro study of mucolytic activity

As demonstrated in two independent studies, the novel SEDDS showed mucus diffusive capacity. The thiolated ingredients, being the single difference between the different

formulations were thus characterized for their muco-interactiv properties, which was assessed rheologically by monitoring the decrease in dynamic viscosity of small intestinal porcine mucus. All tested compounds showed a decrease in dynamic viscosity of mucus over a time period of one hour, leading to decrease in dynamic viscosity of up to 73.4 ± 6.6 % in respect to the negative control, which consisted of mucus and the solubilizing agent EtOH in an equal amount as in the samples (Figure 7). DTT was used in equimolar amount in respect to the free thiol groups of the molecule. Reports about a more pronounced potency of DTT to reduce viscosity of mucus in comparison to NAC led to the choice of DTT as most suitable control [32]. Mucolytic agents expressing a free thiol moiety such as NAC as leading structure are reported to reduce the cross-linking of mucin-fibres by cleaving disulphide bonds and thus reduce the bulk mucus viscosity [16]. The data obtained show a decrease in viscosity for all three molecules, TBA-D, TGA-O and NAC and show structural similarity to NAC by expressing a free thiol group. The mucolytic activity of the novel synthesized excipient is probably based on a disulphide exchange reaction between the thiol-conjugates and the cysteine thiol group in the mucin fibres [5,33,34]. Consequently, the authors assume that the enhancement of droplets diffusion through the mucus is favored due to the incorporated thiol-conjugates.

Computational calculations of the partition coefficients of all used thiolated molecules were calculated by chemsketch [35] (Table 2). The authors assume, that the high partition coefficient of the thiol-conjugates TBA-dodecylamine and TGA-octylamine leads to a stable incorporation of the thiol-conjugates in the SEDDS while the more hydrophilic controls are leaking more quickly giving evidence of a less pronounced and less long lasting effect. The SEDDS droplets, exhibiting a highly lipophilic core, shelter the novel thiol-conjugates, leading to a sustained release due to a leakage of the compounds into the aqueous environment. This continuous and sustained release leads to facilitated mucus permeation, presumable due to a destruction of the mucin network.

4. Conclusion:

Within this study, a potential system to overcome the mucus barrier as critical bottleneck on drug targeting was investigated. This was done by the development of a new generation of SEDDS with mucolytic properties. Incorporation of newly designed thiolated low molecular weight conjugates provided the SEDDS with mucus permeating properties as assessed by MPT studies as well as rotational tube assay. Their high diffusion coefficient in mucus which was faster than that of viruses as well as diffusion in silicone tubes to a greater extent than that of the mucolytic control highlight the potential of the new thiolated SEDDS. Additional rheological studies give proof of the mucolytic activity of the novel thiolated conjugates. The novel thiolated low molecular weight fatty acid derivatives enlarge the field of application of SEDDS for future drug delivery.

Acknowledgement

The authors wish to thank J. Mayr and co-workers from the slaughterhouse Sistrans for supply of porcine intestine.

Financial and competing interests disclosure

The research leading to these results has received funding from the European Community's Seventh Framework Programe [FP7/2007-2013] for ALEXANDER under grant agreement n° NMP-2011-1.2-2-280761.

The authors have no other relevant affiliations or financial involvement with any organization or entity with a financial interest in or financial conflict with the subject matter or materials discussed in the manuscript apart from those disclosed. No writing assistance was utilized in the production of this manuscript.

Tables:

SEDDS	Thiol-conjugate	Zeta potential [mV]	D^{o} [$cm^{2}\ s^{-1}\ x10^{-9}$]	‹Deff› [cm2s-1 $x10^{-9}$]	% Ratio ‹Deff› /D^{o}	% Diffusive droplets
A	TBA-D	-2.1 ± 0.5	101.18	0.87123 ± 0.1223	0.8611	59
B	TGA-O	-2.2 ± 0.4	82.28	0.05135 ± 0.0089	0.0624	35
C	--	-0.8 ± 0.9	122.12	0.01318 ± 0.0003	0.0108	16
NAC	NAC	-7.1 ± 0.2	102.41	0.24624 ± 0.0376	0.2405	40

Table 1: Zeta potential, D° (diffusion coefficient in water), ‹Deff› (diffusion coefficient in mucus) and ratio (%) of diffusive droplets of various SEDDS preparations. Mucus diffusion was measured by MPT technique using the epifluorescence microscopy while diffusion in water was obtained through Stokes-Einstein equation.

molecule	**calculated log P**
TBA-dodecylamine	5.83±0.63
TGA-octylamine	3.14±0.40
NAC	-0.15±-0.47
DTT	0.09±0.71

Table 2: Computational determined log P values as calculated by chemsketch

Figures:

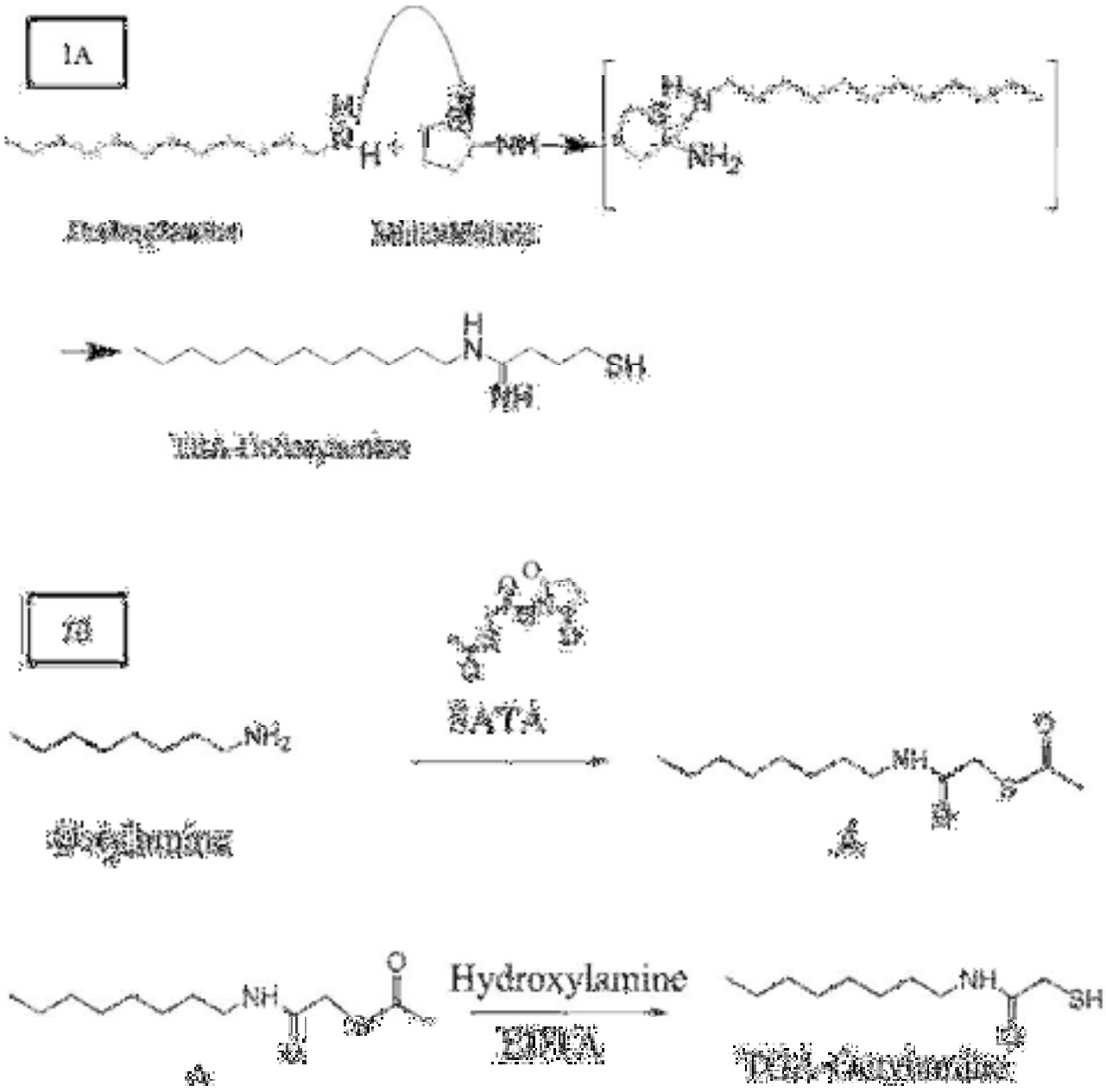

Figure 1 : Postulated reaction scheme for coupling reaction. (1A) Scheme for coupling reaction of dodecylamine with iminothiolane; (1 B) Scheme for coupling reaction of octylamine with SATA

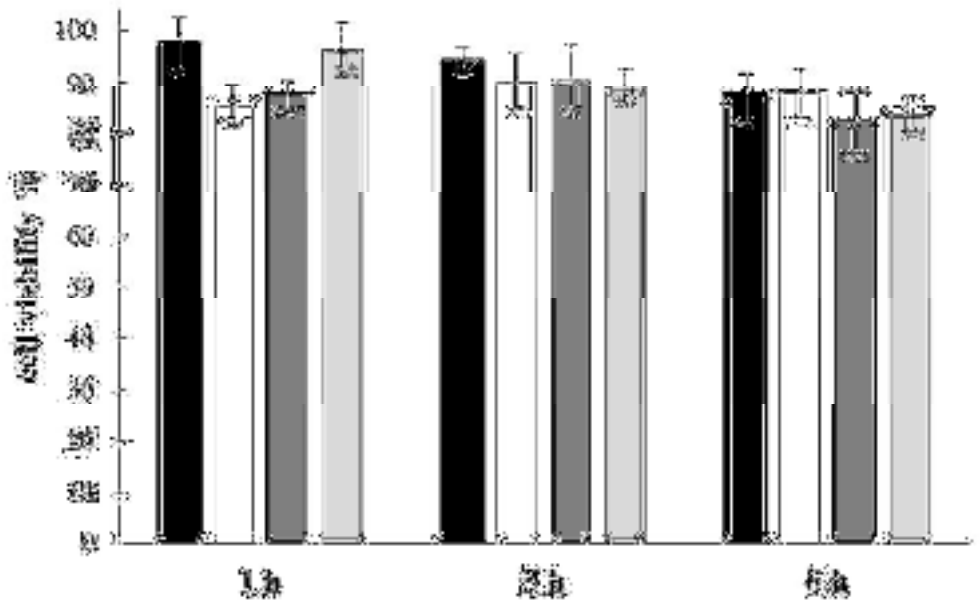

Figure 2: Evaluation of cell viability. The formulations SEDDS A (black bars), SEDDS B (white bars), SEDDS C (dark gray bars) and SEDDS D (bright gray bars)were incubated in a concentration of 0.5 % (m/V) in MEM for up to 6 h. Indicated values are means of at least five experiments (±SD, n=5).

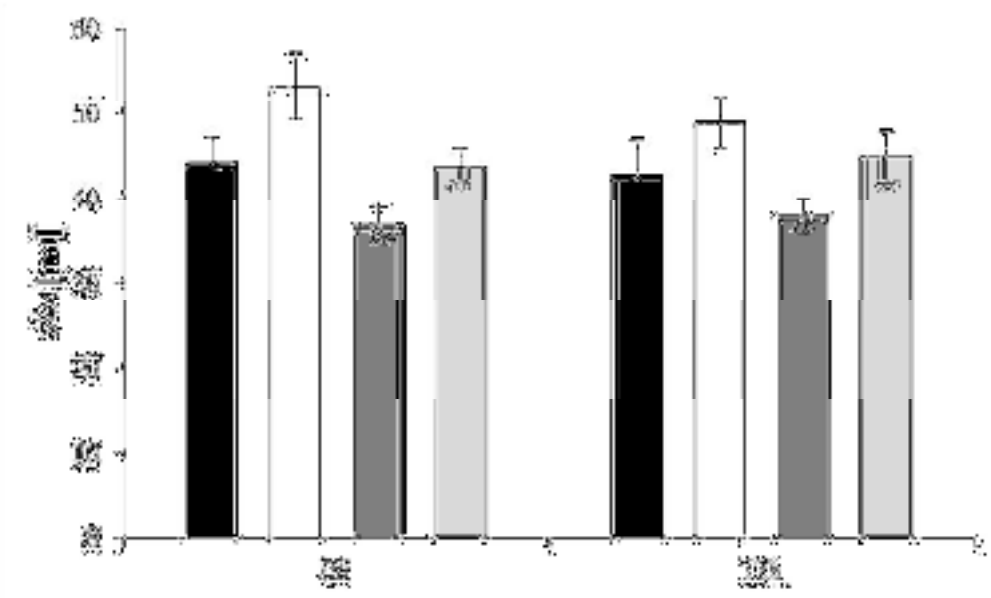

Figure 3: Droplet size of SEDDS loaded with TBA-Dodecylamine (black bars), TGA-Octylamine (white bars) as well as SEDDS without any thiol conjugate (dark grey) and SEDDS loaded with N-acetyl-cysteine (bright grey). The SEDDS were dispersed in bis-tris buffer pH 6.0, 0.1M. Indicated values are mean of at least three experiments (± SD, n=3).

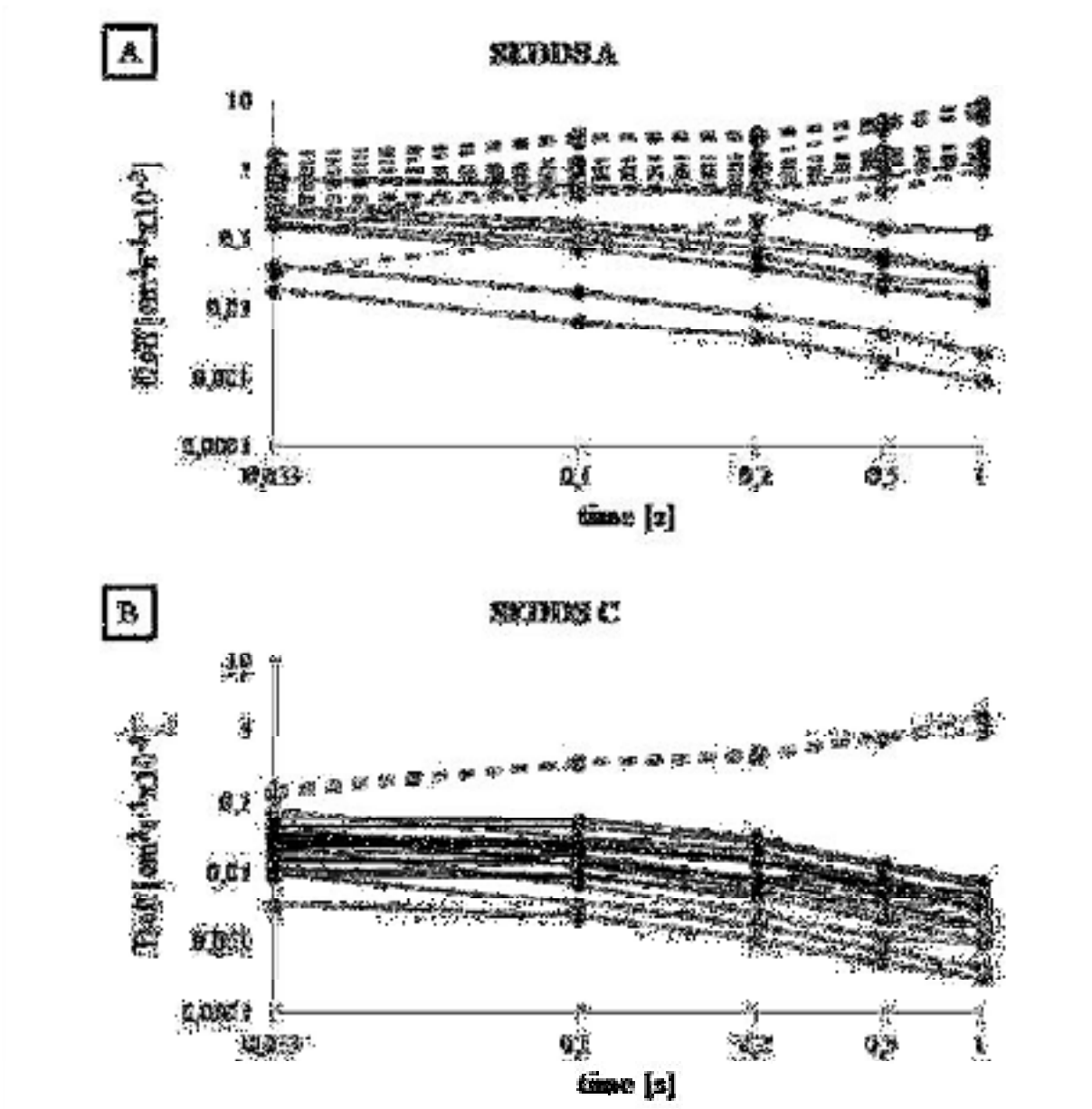

Figure 4: Illustrative profiles for individual effective Diffusion Coefficients (Deff) for each of 20 randomly selected droplets for: (4A) the SEDDS A formulation containing TBA-Dodecylamine, and (4B) the SEDDS C formulation which lacks thiolated compounds. The profiles show discrete measurements for Deff across the entire time interval encompassing the 0.2s and 1s time points. For diffusive droplets the Deff over the period of 1s should decline no lower than 90% of the Deff obtained in the first 0.2s. The profiles clearly show a greater proportion of droplets falling below this requirement for the SEDDS C formulation. The online source random.org was used to randomly select the droplets.

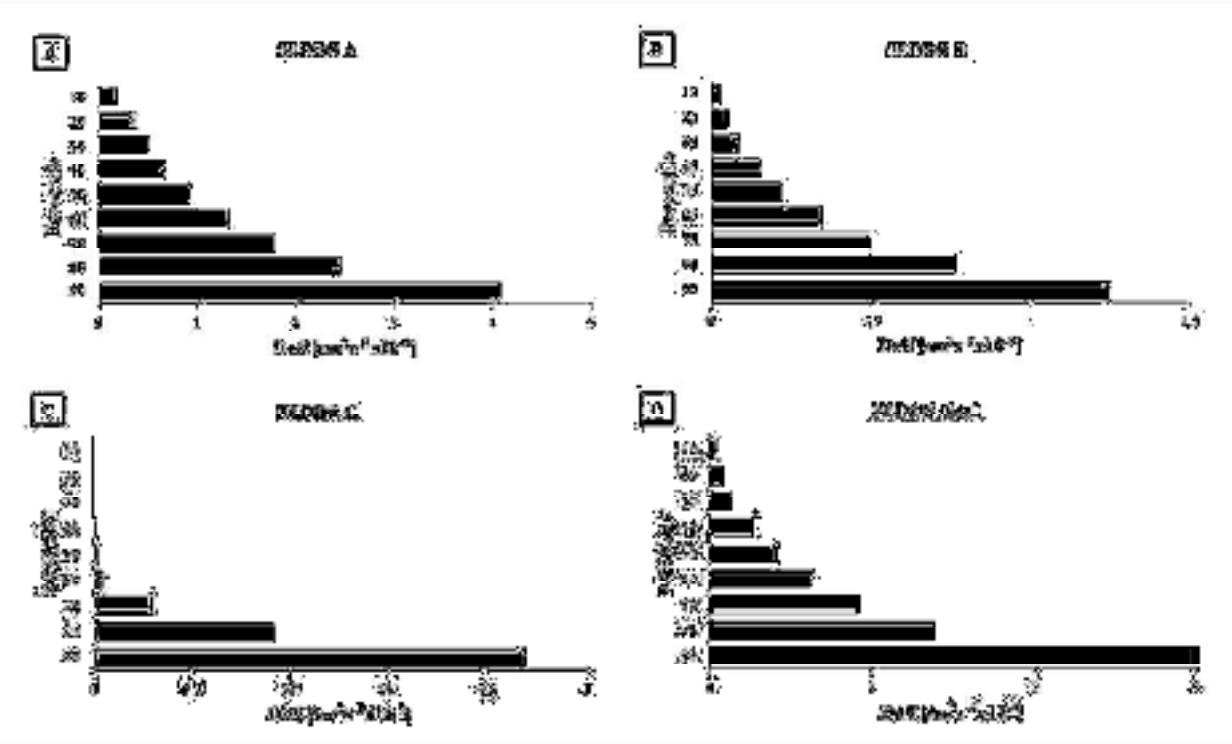

Figure 5: Heterogeneity of droplet movement through mucus. For each droplet type an Effective Diffusion Coefficient ‹Deff› was calculated for each of 360 individual droplets over a time interval of 1s. The data were ranked into percentiles from the 90th through to 10th percentile, where the 90th percentile is the ‹Deff› value below which 90% of the ‹Deff› observations may be found. (A) Data for SEDDS A containing thiobutylamidine-dodecylamine (TBA-Dodecylamine); (B) data for SEDDS B containing thioglycolic-acid-octylamine (TGA-Octylamine); (C) data for reference SEDDS C containing no thiolated compound; (D) data for SEDDS containing N-acetyl-cysteine (NAC). The SEDDS contain 3% of thiolated compound and are prepared in a 1:100 dilution in bis-tris buffer pH 6, 0.1 M. Figure presents data of three separate experiments, i.e. ≥360 individual droplets examined for each droplet type.

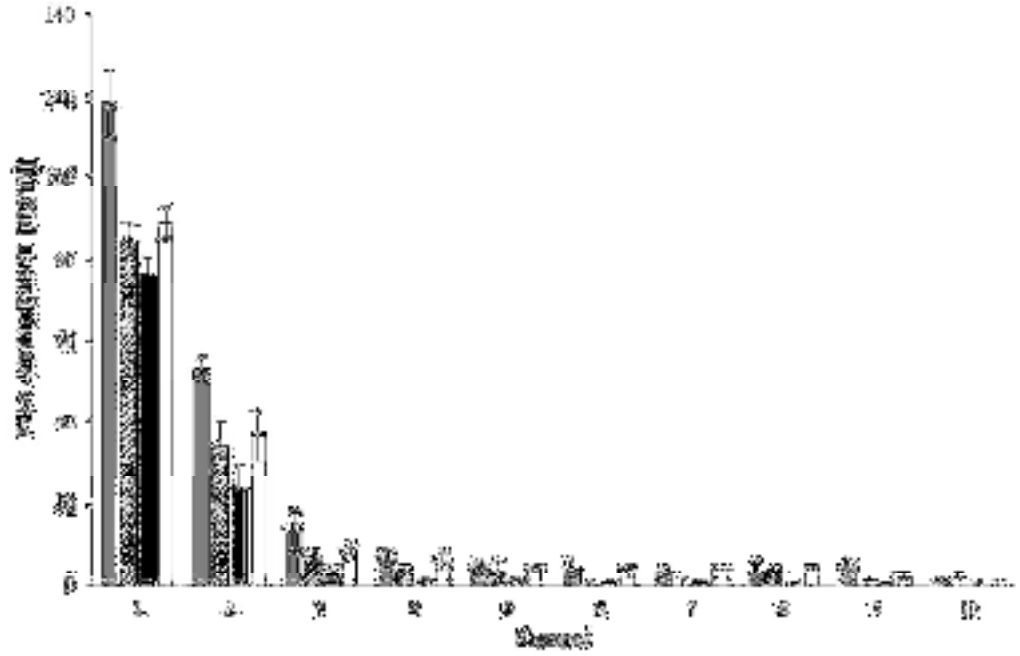

Figure 6: Mucus diffusion study-rotating tubes method. Comparison of FDA concentration in mucus. SEDDS A (dark gray bars), SEDDS B (dashed bars), SEDDS C (black bars) and SEDDS NAC (white bars) in bis tris buffer ph 6.0. Indicated values are means of at least five experiments (± SD, n≥5)

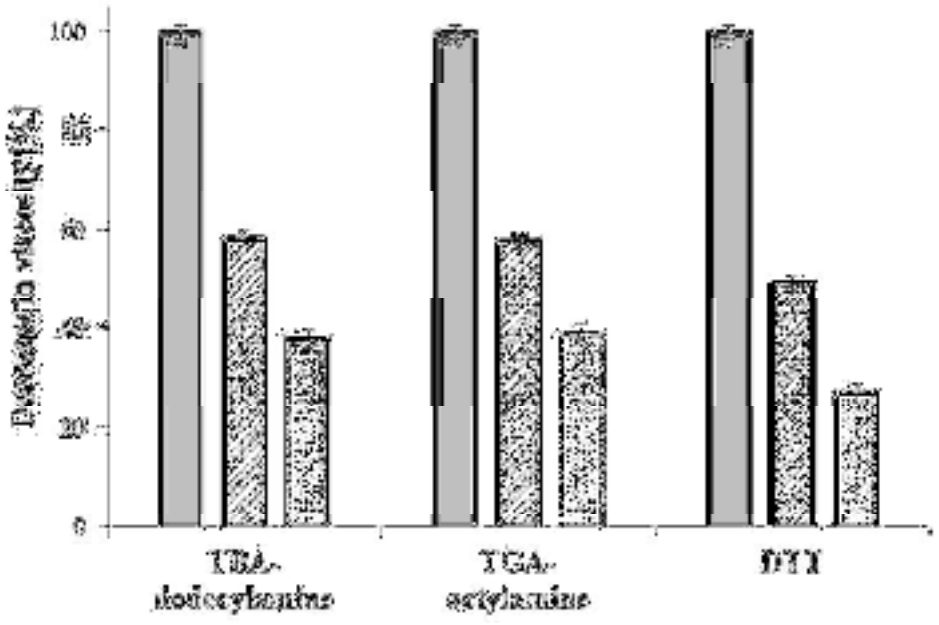

Figure 7: Evaluation of mucolytic effect of TBA-dodecylamine, TGA-octylamine and DTT after 0h (gray bars), 0.5h (dashed gray bars) and 1h (dotted gray bars) used as an ethanolic solution (300 µmol/ml) of thiolated conjugates mixed in a ratio of 1:10 (V/m) with mucus. Mucus containing 10% of EtOH served as negative control. DTT-mucus mixtures prepared in equimolar concentration served as using positive control. Indicated values are means of at least five experiments (±SD, n ≥ 5).

Appendix:

A	^{1}H-NMR spectrum of TBA-D in $CDCl_3$.
B	^{13}C-NMR spectrum of TBA-D in $CDCl_3$.
C	^{1}H-NMR spectrum of TGA-Octylamine-thioester in $CDCl_3$.
D	^{1}H-NMR spectrum of TGA-O in $CDCl_3$.
E	^{13}C-NMR spectrum of TGA-O in $CDCl_3$.
F	Relationship between droplet diameter or zeta potential to droplet diffusion kinetics in mucus. (A) Plot of droplet diameter of the SEDDS versus Effective Diffusion Coefficient ‹Deff›; (B) Plot of zeta potential of the SEDDS versus Effective Diffusion Coefficient ‹Deff›; (C) Plot of zeta potential versus % ratio [‹Deff›]/[D°], a measure of the efficiency of a droplet's diffusion in mucus compared to its diffusion in water. Droplet diameter is expressed in nm, zeta potential is expressed in mV and ‹Deff› is expressed in cm2s-1x10-9.

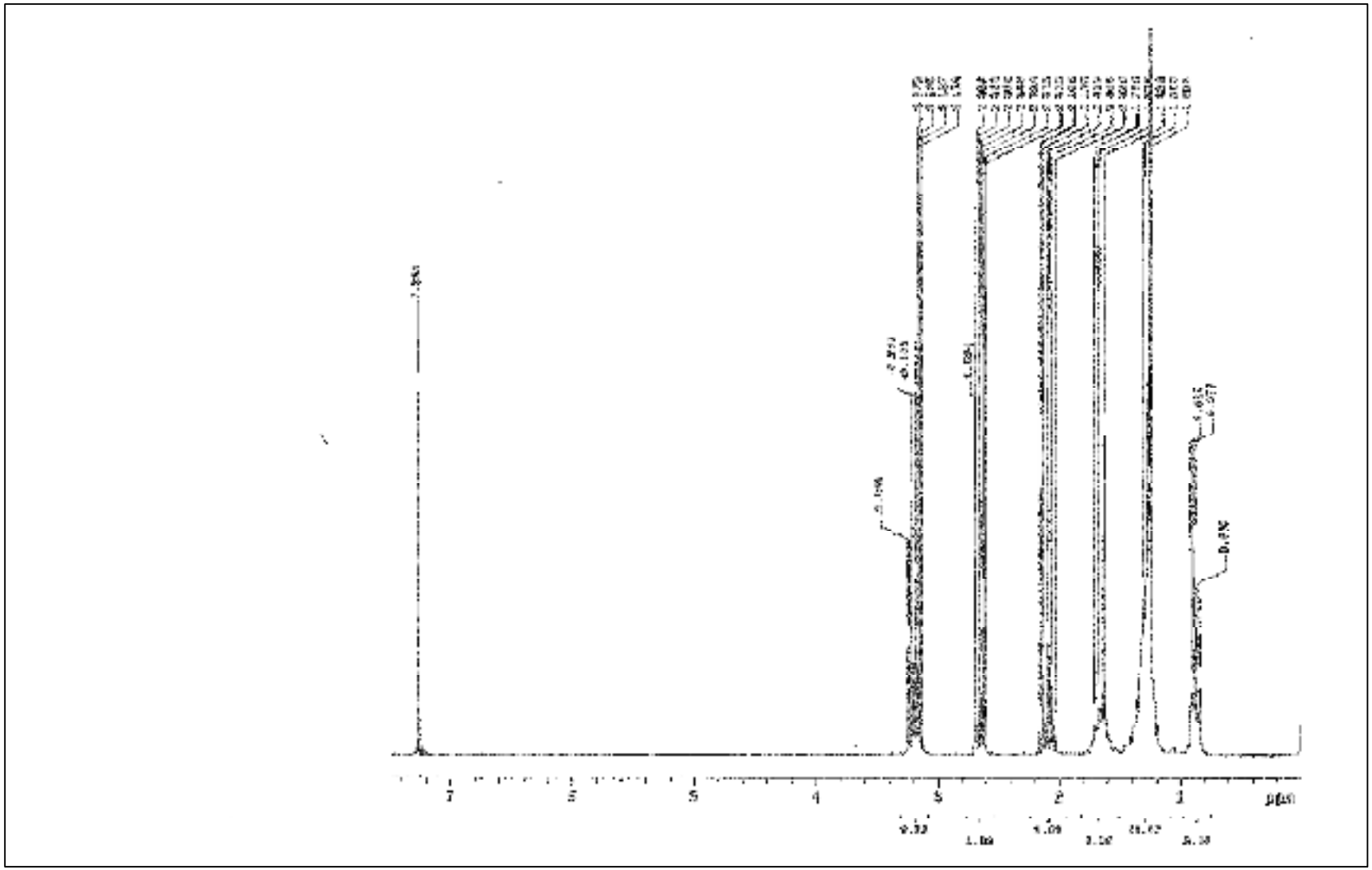

A: ^{1}H-NMR spectrum of TBA-D in $CDCl_3$.

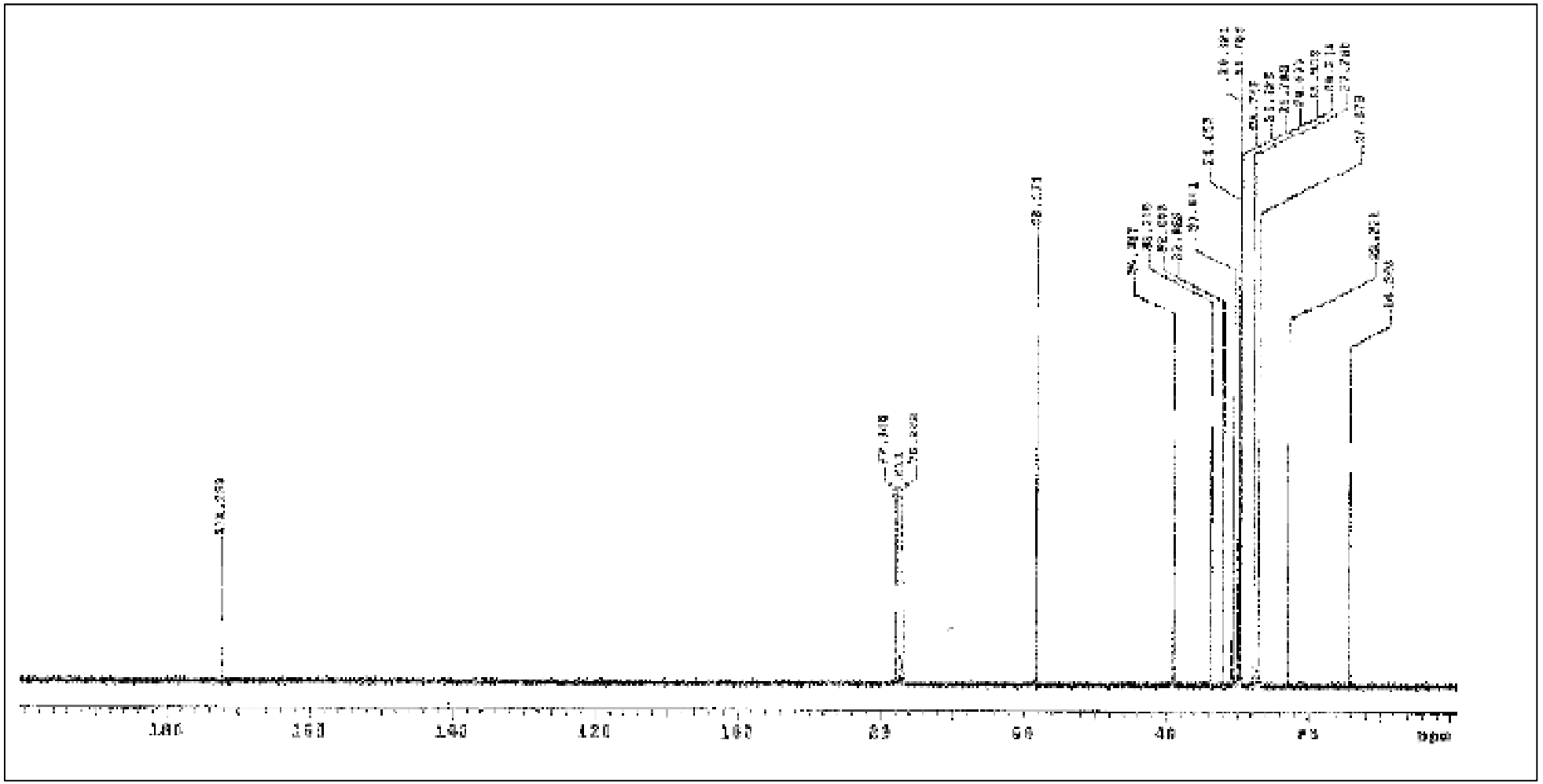

B: ^{13}C-NMR spectrum of TBA-D in $CDCl_3$.

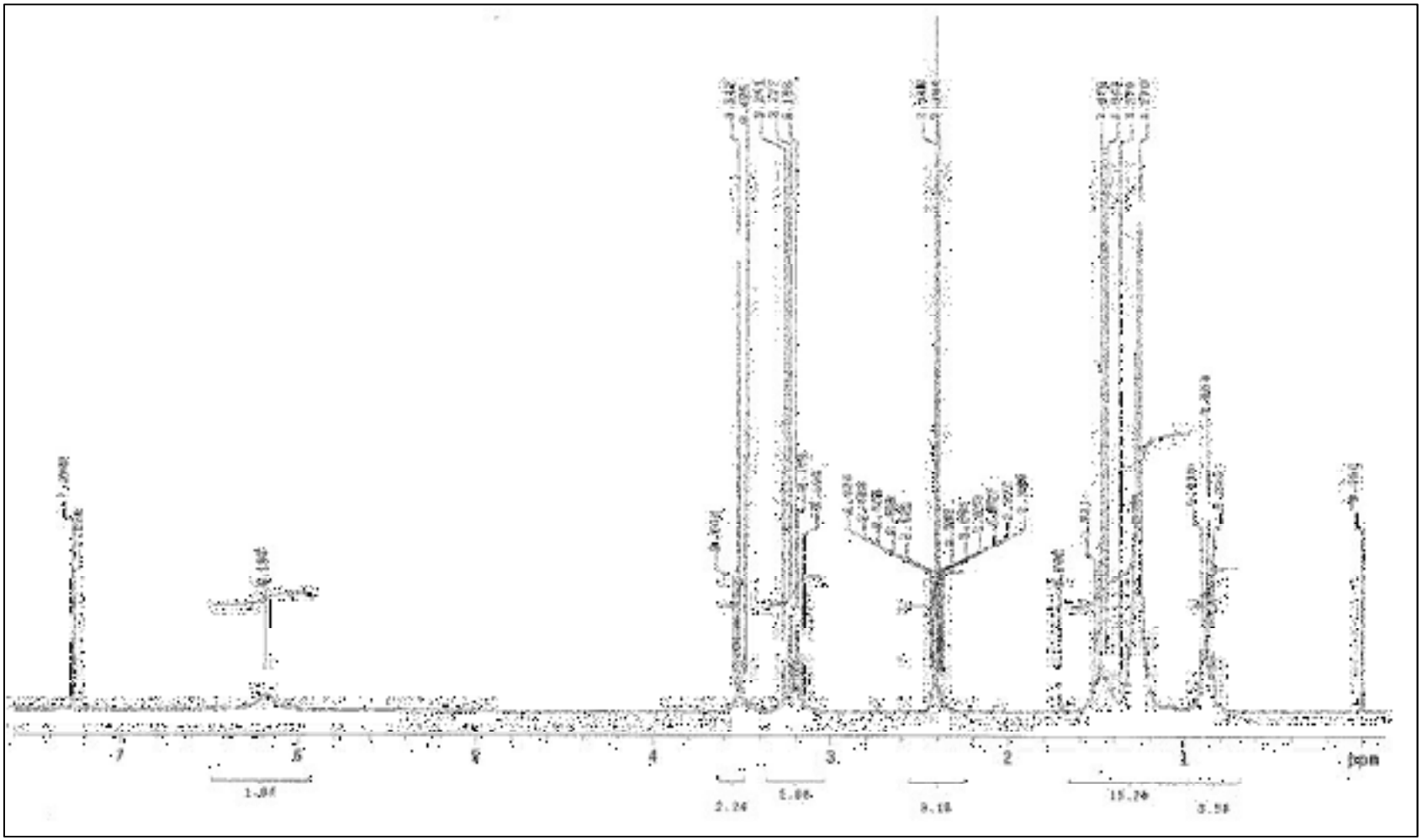

C: ^{1}H-NMR spectrum of TGA-Octylamine-thioester in $CDCl_3$.

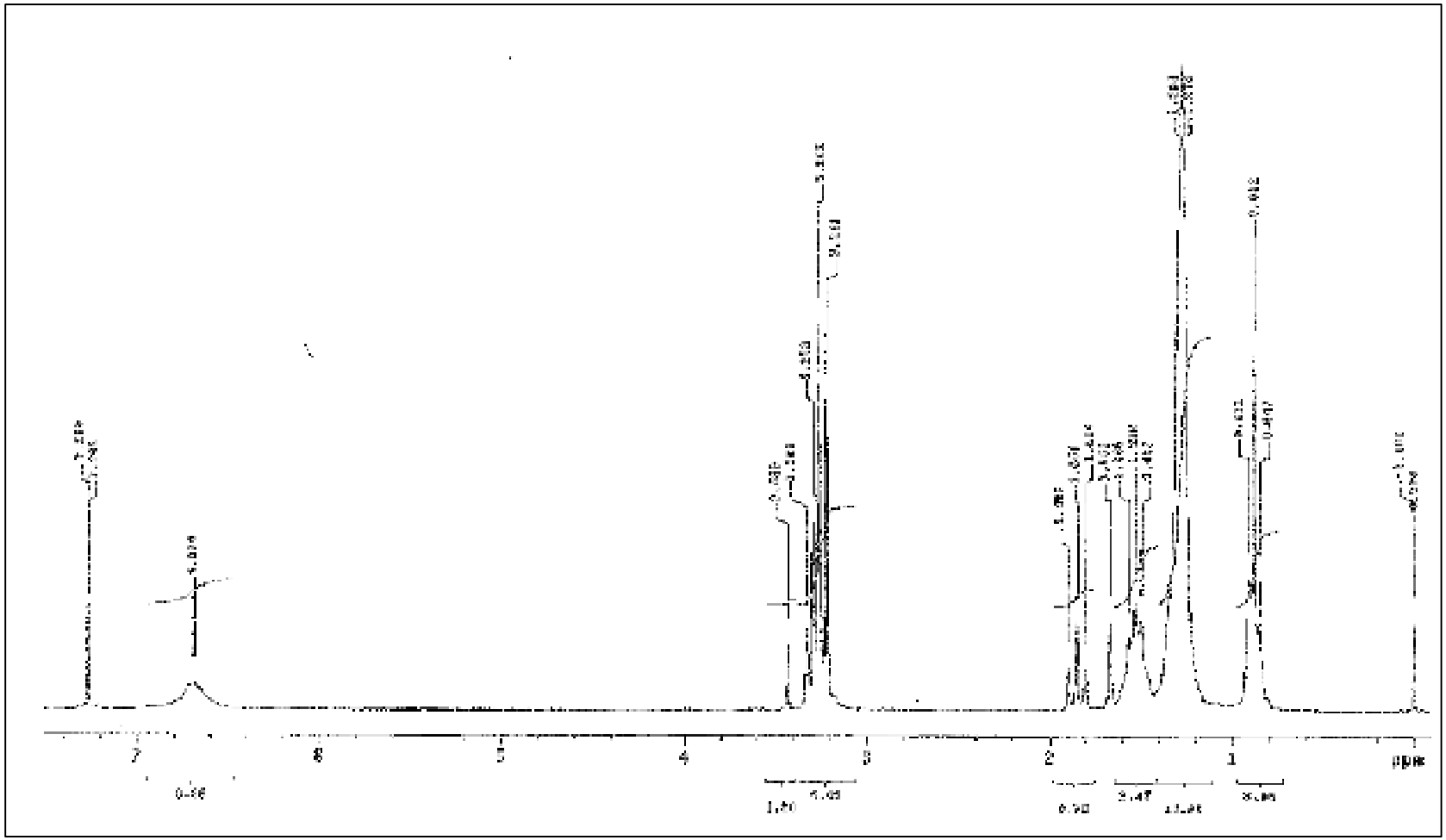

D: ^{1}H-NMR spectrum of TGA-O in $CDCl_3$.

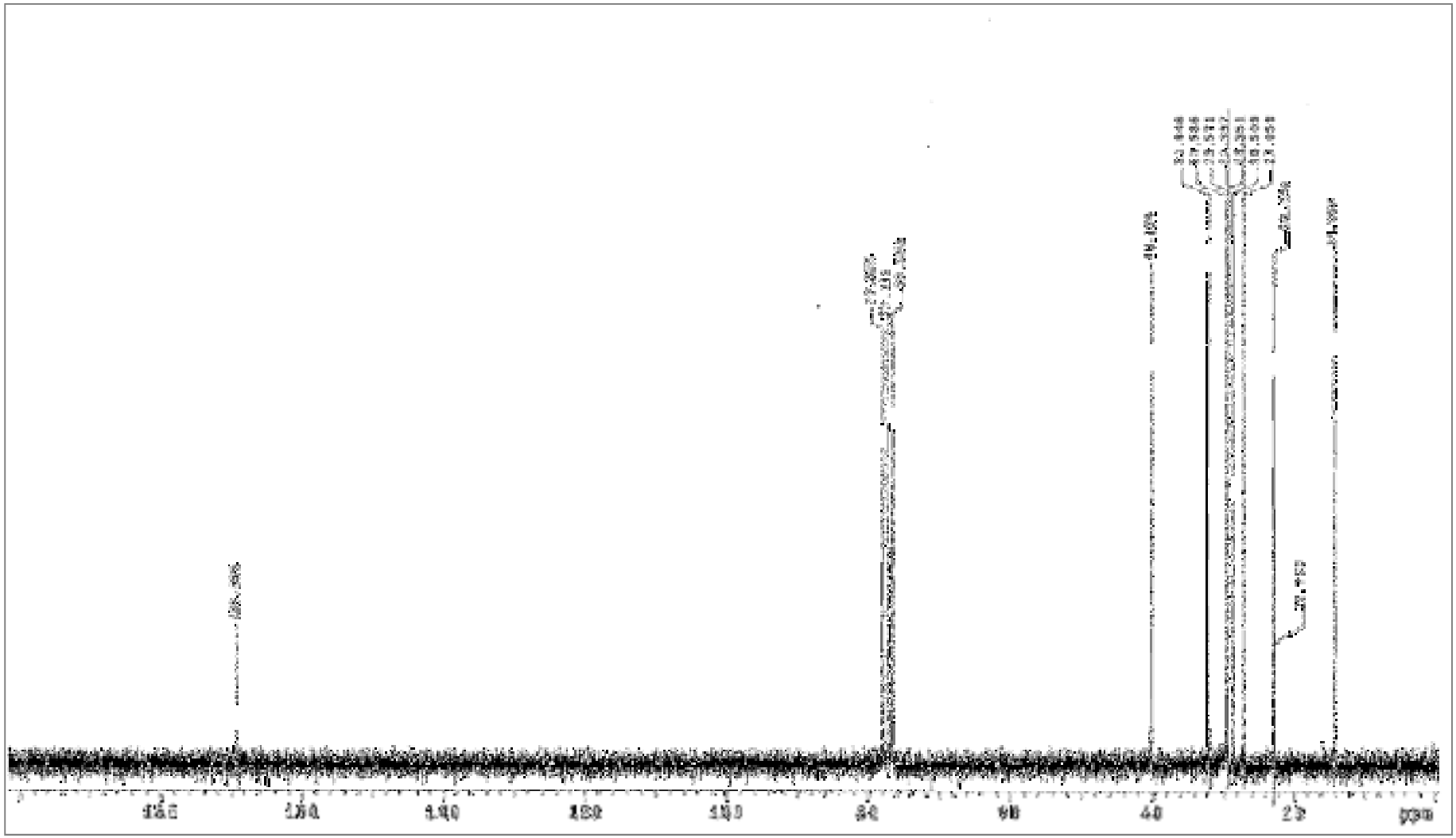

E: ^{13}C-NMR spectrum of TGA-O in $CDCl_3$

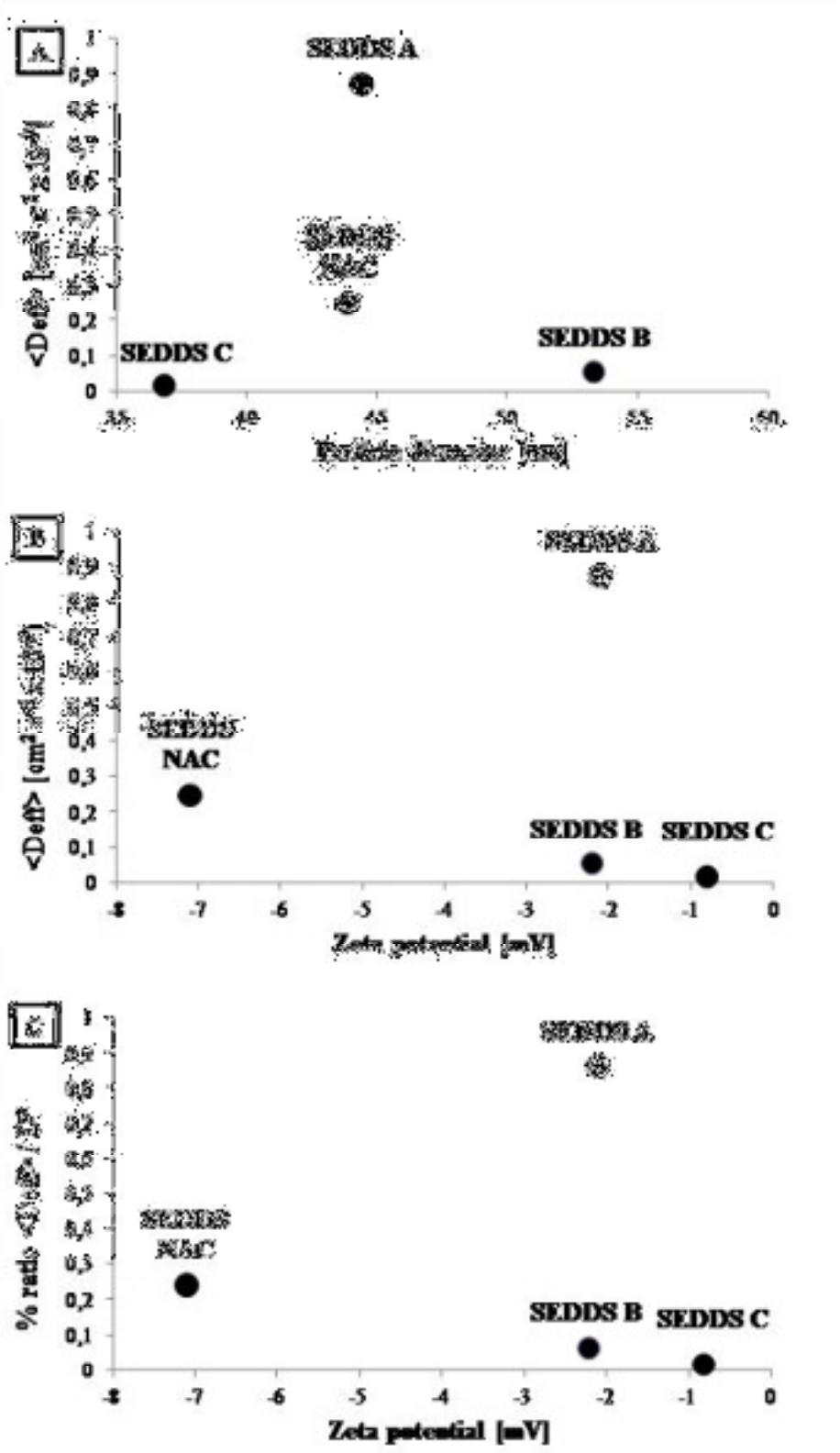

F: Relationship between droplet diameter or zeta potential to droplet diffusion kinetics in mucus. (A) Plot of droplet diameter of the SEDDS versus Effective Diffusion Coefficient ‹Deff›; (B) Plot of zeta potential of the SEDDS versus Effective Diffusion Coefficient ‹Deff›; (C) Plot of zeta potential versus % ratio [‹Deff›]/[D°], a measure of the efficiency of a droplet's diffusion in mucus compared to its diffusion in water. Droplet diameter is expressed in nm, zeta potential is expressed in mV and ‹Deff› is expressed in cm2s-1x10-9.

References

[1] Atuma C, Strugala V, Allen A, Holm L. The adherent gastrointestinal mucus gel layer: thickness and physical state in vivo. American Journal of Physiology-Gastrointestinal and Liver Physiology 2001;280:G922-G929.

[2] Cone RA. Barrier properties of mucus. Advanced Drug Delivery Reviews 2009;61:75–85.

[3] Ensign LM, Cone R, Hanes J. Oral drug delivery with polymeric nanoparticles: the gastrointestinal mucus barriers. Adv Drug Deliv Rev 2012;64:557–70.

[4] Turner JR. Intestinal mucosal barrier function in health and disease. Nat Rev Immunol 2009;9:799–809.

[5] Suk JS, Lai SK, Boylan NJ, Dawson MR, Boyle MP, Hanes J. Rapid transport of muco-inert nanoparticles in cystic fibrosis sputum treated with N-acetyl cysteine. Nanomedicine 2011;6:365–75.

[6] Dünnhaupt S, Kammona O, Waldner C, Kiparissides C, Bernkop-Schnürch A. Nano-carrier systems: Strategies to overcome the mucus gel barrier. European Journal of Pharmaceutics and Biopharmaceutics; doi:10.1016/j.ejpb.2015.01.022; in press

[7] Köllner S, Dünnhaupt S, Waldner C, Hauptstein S, Pereira de Sousa I, Bernkop-Schnürch A. Mucus permeating thiomer nanoparticles. European Journal of Pharmaceutics and Biopharmaceutics; doi:10.1016/j.ejpb.2015.01.004; in press

[8] Wilcox MD, van Rooij LK, Chater PI, Pereira de Sousa I, Pearson JP. The effect of nanoparticle permeation on the bulk rheological properties of mucus from the small intestine. European Journal of Pharmaceutics and Biopharmaceutics; doi:10.1016/j.ejpb.2015.02.029; in press

[9] Wang Y, Lai SK, Suk JS, Pace A, Cone R, Hanes J. Addressing the PEG mucoadhesivity paradox to engineer nanoparticles that “slip” through the human mucus barrier. Angewandte Chemie International Edition 2008;47:9726–9.

[10] Bonengel S, Prüfert F, Perera G, Schauer J, Bernkop-Schnürch A. Polyethylene imine-6-phosphogluconic acid nanoparticles – a novel zeta potential changing system. International Journal of Pharmaceutics 2015;483:19–25.

[11] Friedl H, Dünnhaupt S, Hintzen F, Waldner C, Parikh S, Pearson JP, Wilcox MD et al. Development and Evaluation of a Novel Mucus Diffusion Test System Approved by Self-Nanoemulsifying Drug Delivery Systems. Journal of pharmaceutical sciences 2013;102:4406–13.

[12] Constantinides PP. Lipid microemulsions for improving drug dissolution and oral absorption: physical and biopharmaceutical aspects. Pharmaceutical research 1995;12:1561–72.

[13] Pouton CW. Formulation of self-emulsifying drug delivery systems. The Potential of Oily Formulations for Drug Delivery to the Gastro-intestinal Tract 1997;25:47–58.

[14] Lai SK, Wang Y, Hanes J. Mucus-penetrating nanoparticles for drug and gene delivery to mucosal tissues. Advanced Drug Delivery Reviews 2009;61:158–71.

[15] Abdulkarim M, Agullo N, Cattoz B, Griffiths P, Bernkop-Schnurch A, Borros SG, Gumbleton M. Nanoparticle diffusion within intestinal mucus: Three-dimensional response analysis dissecting the impact of particle surface charge, size and heterogeneity across polyelectrolyte, pegylated and viral particles. Eur J Pharm Biopharm 2015; doi:10.1016/j.ejpb.2015.01.023; in press

[16] Hintzen F, Laffleur F, Sarti F, Müller C, Bernkop-Schnürch A. In vitro and ex vivo evaluation of an intestinal permeation enhancing self-microemulsifying drug delivery system (SMEDDS). Journal of Drug Delivery Science and Technology 2013;23:261–7.

[17] Partenhauser A, Laffleur F, Rohrer J, Bernkop-Schnürch A. Thiolated silicone oil: Synthesis, gelling and mucoadhesive properties. Acta Biomaterialia 2015;16:169–77.

[18] O'Brien J, Wilson I, Orton T, Pognan F. Investigation of the Alamar Blue (resazurin) fluorescent dye for the assessment of mammalian cell cytotoxicity. European Journal of Biochemistry 2000;267:5421–6.

[19] MacAdam A. The effect of gastro-intestinal mucus on drug absorption. Relevance of Mucus to Advanced Drug Delivery 1993;11:201–20.

[20] Hanes J, Lai SK. Compositions and methods for enhancing transport through mucus: Google Patents; 2007.

[21] Apgar J, Tseng Y, Fedorov E, Herwig MB, Almo SC, Wirtz D. Multiple-particle tracking measurements of heterogeneities in solutions of actin filaments and actin bundles. Biophysical Journal 2000;79:1095–106.

[22] Lai SK, O'Hanlon DE, Harrold S, Man ST, Wang Y, Cone R, Hanes J. Rapid transport of large polymeric nanoparticles in fresh undiluted human mucus. Proc Natl Acad Sci U S A 2007;104:1482–7.

[23] Macierzanka A, Mackie AR, Bajka BH, Rigby NM, Nau F, Dupont D. Transport of Particles in Intestinal Mucus under Simulated Infant and Adult Physiological Conditions: Impact of Mucus Structure and Extracellular DNA. PloS one 2014;9:e95274.

[24] Philibert J. One and a half century of diffusion: Fick, Einstein, before and beyond. Diffusion Fundamentals 2005;2:1–10.

[25] Dünnhaupt S, Barthelmes J, Hombach J, Sakloetsakun D, Arkhipova V, Bernkop-Schnurch A. Distribution of thiolated mucoadhesive nanoparticles on intestinal mucosa. Int J Pharm 2011;408:191–9.

[26] Sakloetsakun D, Hombach JMR, Bernkop-Schnürch A. In situ gelling properties of chitosan-thioglycolic acid conjugate in the presence of oxidizing agents. Biomaterials 2009;30:6151–7.

[27] Norris DA, Puri N, Sinko PJ. The effect of physical barriers and properties on the oral absorption of particulates. Oral Particulates 1998;34:135–54.

[28] Lai SK, Wang Y, Hida K, Cone R, Hanes J. Nanoparticles reveal that human cervicovaginal mucus is riddled with pores larger than viruses. Proceedings of the National Academy of Sciences 2010;107:598–603.

[29] Allen A, Snary D. The structure and function of gastric mucus. Gut 1972;13:666–72.

[30] Dawson M, Wirtz D, Hanes J. Enhanced viscoelasticity of human cystic fibrotic sputum correlates with increasing microheterogeneity in particle transport. J Biol Chem 2003;278:50393–401.

[31] Božič AL, Šiber A, Podgornik R. How simple can a model of an empty viral capsid be? Charge distributions in viral capsids. Journal of biological physics 2012;38:657–71.

[32] McNiff E, Clemente E, Fung H. In-Vitro Comparison of the Mucolytic Activity of Sodium Metabisulfite, N-Acetylcysteine and Dithiothreitol. Drug Development and Industrial Pharmacy 1974;1:507–16.

[33] Sheffner AL. The reduction in vitro in viscosity of mucoprotein solutions by a new mucolytic agent N-acetyl-L-cysteine. Annals of the New York Academy of Sciences 1963;106:298–310.

[34] Stey C, Steurer J, Bachmann S, Medici TC, Tramer. The effect of oral N-acetylcysteine in chronic bronchitis: a quantitative systematic review. European Respiratory Journal 2000;16:253–62.

[35] Tetko IV, Gasteiger J, Todeschini R, Mauri A, Livingstone D, Ertl P, Palyulin VA et al. Virtual computational chemistry laboratory–design and description. Journal of computer-aided molecular design 2005;19:453–63.